

Coherent manipulation for creating two spin entanglement by moving magnetic tip

Qing Ai,¹ Yong Li,² Guilu Long,^{1,3} and C. P. Sun⁴

¹*Department of Physics, Tsinghua University, Beijing 100084, China*

²*Department of Physics and Astronomy, University of Basel, Klingelbergstrasse 82, 4056 Basel, Switzerland*

³*Tsinghua National Laboratory for Information Science and Technology, Beijing 100084, China*

⁴*Institute of Theoretical Physics, Chinese Academy of Sciences, Beijing, 100080, China*

We theoretically explore the possibility of simultaneously coupling the two local spins by generalizing the time-dependent Fröhlich coupling by microscopically modeling the tip as a harmonic oscillator, or a single mode localized in the two quantum dots. The state based architecture for cavity QED will result in an effective interaction between the tip, a maximum entangled state and the horizontal distance between the two qubits. The created entanglement depends on the quantum entanglement induced by the accelerated motion while it is not for the

PACS numbers: 03.67.Lx,07.79.Cz

I. INTRODUCTION

Since Shor and Grover algorithms [2, 3] were proposed, with various following significant developments, especially the quantum computing has been displaying its more amazing charm against classical computation. More progress has been made in this area, it is to discover various robust, controllable and scalable level systems - qubits as the basic elements for the architecture of quantum computers. In usual, electron spins are a natural qubit, especially the single electron spin confined in a quantum dot for its well separability and easy addressability. In Ref.[5], electron spins in quantum dots were employed as qubits and two-qubit operations were performed by pulsing the electrostatic barrier between neighboring spins. Thereafter, Kane's model made use of the nuclear spins of ³¹P donor impurities as qubits [6]. It combined the long decoherence of nuclear spins and the advantage of the well developed modern semiconductor industry.

However, it seems difficult to control the coupling between qubits because the coupling is based on the overlap of two adjacent spin wave functions [5, 6] and given to be fixed once photolithography of the circuit has been finished. Moreover, inspired by the development of single spin detection [7], Berman *et al.* developed a model of quantum computing by scanning tunneling microscopy (STM)[8, 9]. Long *et al.* proposed a quantum computing scheme also using a STM with a moving tip as a commuter to perform the control-not gate between two qubits on the silicon surface [10]. Here, the tip plays the role of the quantum data bus to coherently link to the qubits.

We notice that the moving tip essentially is a quantized

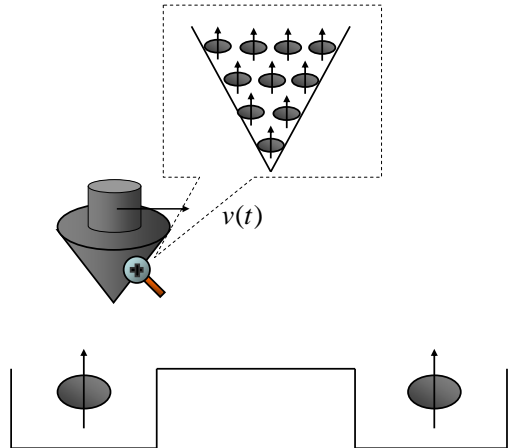


FIG. 1: (Color Online) Schematic of two single-electron quantum dots and a moving magnetic tip. Two single-electron quantum dots are placed at the surface of the solid. The tip, originally located above electron 1, moves towards electron 2.

harmonic oscillator, which can be experimentally realized by the nanometer scale nanomechanical resonator (NAMR) with GHz frequency oscillation [11, 12, 13, 14, 15]. To show an artificial cavity quantum electrodynamics (QED) structure based on the coupling of spin to the NAMR, where the quantized phonon excitation of the NAMR plays the role of a single mode boson field in the conventional cavity QED. To coherently link more qubits and then to induce the quantum entanglements of these qubits, the NAMR can behave as the quantum data bus. It is noticed that the quantization of NAMR or the moving

ing tip is crucial to entangle qubits. Fortunately, been theoretically shown that, in principle, the tip could be cooled into the quantum regime [16], i.e. standard quantum limit. Now, we can make an improved quantization of the moving tip since we can simply model the tip as an ensemble of many spins. This model approach is supported by the theoretical and experimental investigations about the nanomechanical system cavity QED.

Actually several recent experiments have been performed to show the quantum coherent phenomena caused by the interaction between an electron spin and an ensemble of nuclei spins [17, 18, 19, 20]. When an electron is coupled with an ensemble of N nuclear spins, the collective coupling intensity is increased by a factor N [21]. With these enhanced interactions, it is more difficult to manipulate spins fast with a tip consisting of many spins. Indeed, when the couplings of the spin and nuclear ensemble are quasi-homogeneous, the interaction between the electron spin and the collective excitation of nuclei spins can be well described in terms of an artificial cavity QED [22]. Here, the collective excitation can be treated as a single mode boson for quantum data bus and the electron spin acts as a two-level artificial atom. It is this exploration that motivates us to further propose a microscopic model for two or more spin entanglement induced by an effective quantum data bus, the collective excitation of the many spin tip.

In our model, two electrons are confined in two single electron quantum dots respectively, while a tip is moving above them (see Fig.1). With the frequency selection for the resonance effect, there is only one mode of collective excitations interacting with the two spins. Especially, when the Zeeman splits of all nuclear spins are the same, the single mode excitation can decouple with other modes [22]. Then, the coupling system with two qubit spins and a tip just acts as typical cavity QED system or spin-boson system. To coherently manipulate the indirect interaction between the two spins, which is induced by the above mentioned collective excitation, we need to move the tip for switching on and off such interaction to realize a two qubit logical gate operation. Since the moving of the tip leads to a time-dependent coupling, we need to use some new method to derive the effective Hamiltonian for the inter-spin coupling. Fortunately, a recent paper suggested such time-dependent approach [1].

The rest of our paper is organized as follows. In Sec.II we simplify the total system as two spins interacting with a single mode of the collective excitation of the tip to form a cavity-QED under the homogeneous condition. In Sec. III we derive the effective Hamiltonian between the two electron spins by the time-dependent Fröhlich transformation (TDFT) method developed most recently [1]. We remark that the TDFT method can be used to derive an effective Hamiltonian for a class of cavity QED systems with time-dependent perturbations. Here, we use such a transformation for the case with time-dependent couplings of two spins to a many spin ensemble. Section IV

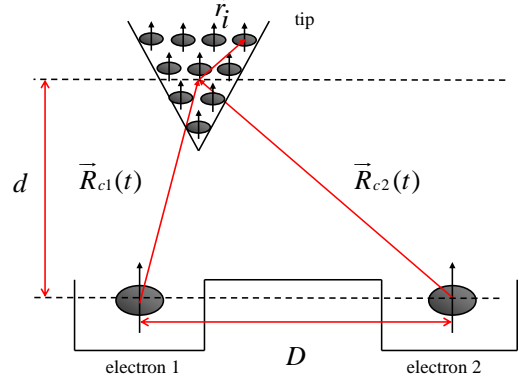


FIG. 2: Schematic of the tip's position with respect to the two electrons. $\vec{R}_{c1}(t)$ ($\vec{R}_{c2}(t)$) is the position of the tip center with respect to electron 1(2), \vec{r}_i is the position of i 'th nuclear spin with respect to the tip center, d is the vertical distance between the tip center and electron 1 (2), D is the horizontal distance between the two electrons.

contains the discussion of entanglement induced by the effective Hamiltonian and different motion types' effect on the entanglement. In Sec. V we review most of the significant results. Finally, technical details are given in Appendices A-C.

II. MODEL DESCRIPTION

We consider the model illustrated in Fig.1 and Fig.2. Two single electron quantum dots with the horizontal distance D are placed at the surface. A tip composed of N nuclear spins is initially located above electron 1. The position of i 'th nuclear spin is \vec{r}_i with respect to the center of the tip. As the tip is horizontally moving over the surface, the position of the tip center with respect to electron 1 (2) is denoted by a time-dependent position vector $\vec{R}_{c1}(t)$ ($\vec{R}_{c2}(t)$). In this model, the vertical distance between the tip center and electron 1 (2) d is fixed when the tip is moving. Thus, when a static magnetic field is applied to the total system, the Hamiltonian reads as

$$H^S = \Omega_z(S_z^{(1)} + S_z^{(2)}) + \omega_z \sum_{j=1}^N I_z^{(j)} + S_z^{(1)} \sum_{j=1}^N g_1^{(j)} I_z^{(j)} + S_z^{(2)} \sum_{j=1}^N g_2^{(j)} I_z^{(j)} + S_+^{(1)} \sum_{l=1}^N \frac{g_1^{(j)}}{2} I_{\pm}^{(j)} + S_+^{(2)} \sum_{l=1}^N \frac{g_2^{(j)}}{2} I_{\pm}^{(j)} + h.c., \quad (1)$$

where $S_z^{(l)}$ and $S_{\pm}^{(l)}$ ($= S_x^{(l)} \pm iS_y^{(l)}$) ($l = 1, 2$) are the spin operators for the l 'th electron spin, $I_z^{(j)}$ and $I_{\pm}^{(j)}$ ($= I_x^{(j)} \pm iI_y^{(j)}$) ($j = 1, 2, \dots, N$) the spin operators for the j 'th

nuclear spins. The first and second terms of Hamiltonian (1) are the Zeeman energies for the electron spins and the nuclear spins respectively, and the terms behind them are the hyperfine interaction between the electrons and nuclear spins. Generally speaking, the constant for the hyperfine interaction, e.g., $g_1^{(i)}$, is an anisotropic tensor [26]. Without loss of generality, we assume it to be a scalar. Therefore, $g_1^{(i)}$ and $g_2^{(i)}$ become

$$g_1^{(i)} \simeq g_0 f_1(t), g_2^{(i)} \simeq g_0 f_2(t).$$

For the necessary details please refer to the Appendix A. Here, the profiles of couplings are

$$f_1(t) = e^{-\alpha|\vec{R}_{c1}(t)|} = e^{-\alpha\sqrt{d^2+R(t)^2}}, \quad (2)$$

$$f_2(t) = e^{-\alpha|\vec{R}_{c2}(t)|} = e^{-\alpha\sqrt{d^2+[D-R(t)]^2}} \quad (3)$$

with $\alpha = 2/a$ (a is the Bohr radius for the electron in the quantum dot) and $R(t)$ being the horizontal distance between electron 1 and the tip center, $g_0 \simeq 120$ Hz.

We have assumed the distances between the electrons and the center of the tip are much larger than the distribution of the nucleus around the tip center,

$$|\vec{R}_{c1}(t)| \gg |\vec{r}_i|, |\vec{R}_{c2}(t)| \gg |\vec{r}_i|.$$

It is a reasonable approximation since for a cubic tip containing $N = 100$ atoms the maximum distance between the atoms and the tip center is about

$$\begin{aligned} \max\{|\vec{r}_i|\} &\simeq \sqrt[3]{N}a_0/2 \\ &\simeq 0.11 \text{ nm} \ll d = 1 \text{ nm}, \end{aligned}$$

where d is the minimum value for $|\vec{R}_{c1}(t)|$ and $|\vec{R}_{c2}(t)|$ (d is also the vertical component for $\vec{R}_{c1}(t)$ and $\vec{R}_{c2}(t)$). Here, the Bohr radius of a hydrogen atom a_0 is considered as the order of the size of a nuclear spin. Besides, there is no direct interaction between two electrons since there is no significant electron wavefunction overlap as $D \gg a$.

In Ref.[22], the collective excitation of an ensemble of polarized nuclei fixed in a quantum dot was studied. Under the approximately homogeneous condition the many-particle system behaves as a single-mode boson interacting with the spin of a single conduction-band electron confined in this quantum dot. Since the homogeneous condition is fulfilled after the approximation made above, the same method in Ref.[22] can be applied to our model. First of all, we introduce a pair of collective operators

$$B = \frac{\sum_{i=1}^N I_-^{(i)}}{\sqrt{2NI_0}} \quad (4)$$

and its conjugate B^+ to depict the collective excitations in the ensemble of nuclei with spin I_0 from its polarized initial state

$$|G\rangle = \prod_{i=1}^N |-I_0\rangle_i \quad (5)$$

which is the saturated ferromagnetic state of nuclei ensemble. It was proved that the collective excitation described by B can behave as a boson mode in the large N limit with an initial polarization of all spins in ground (spin down) state.

In addition to the basic mode denoted by B and B^+ , auxiliary modes

$$C_k = \frac{\sum_{i=1}^N h_i^{[k]} I_-^{(i)}}{\sqrt{2I_0(\vec{h}^{[k]})^2}} \quad (6)$$

(for $k = 1, 2, \dots, N$), where

$$\vec{h}^{[k]} = (h_1^{[k]}, h_2^{[k]}, \dots, h_N^{[k]})$$

are N orthogonal vectors in N -dimensional space \mathbf{R}^N , which can be systematically constructed by making use of the Gramm-Schmidt orthogonalization method starting from

$$\vec{h}^{[1]} = (g_1, g_2, \dots, g_N) \in \mathbf{R}^N.$$

Therefore, the Hamiltonian (1) shall be rewritten as

$$\begin{aligned} H^S \simeq & f_1 \Omega (S_+^{(1)} B + S_-^{(1)} B^+) + f_2 \Omega (S_+^{(2)} B + S_-^{(2)} B^+) \\ & + (\Omega_z - f_1 N g_0 I_0) S_z^{(1)} + (\Omega_z - f_2 N g_0 I_0) S_z^{(2)} \\ & + \omega_z \sum_k C_k^+ C_k + \omega_z B^+ B + H_p^S, \end{aligned} \quad (7)$$

where the effective Rabi frequency is

$$\Omega = g_0 \sqrt{\frac{1}{2} NI_0}$$

and the single particle excitation perturbation

$$\begin{aligned} H_p^S &= g_0 (S_z^{(1)} f_1 + S_z^{(2)} f_2) \sum_i (I_z^{(i)} + I_0) \\ &= g_0 (S_z^{(1)} f_1 + S_z^{(2)} f_2) (B^+ B + \sum_k C_k^+ C_k) \end{aligned} \quad (8)$$

includes the coupling between electrons and C_k modes and can be treated as a perturbation term in the low-excitation limit.

III. EFFECTIVE INTER-SPIN COUPLING DESCRIPTION

As shown in Hamiltonian (7), there are only couplings of two electron spins with the single mode boson respectively. By making use of the canonical transformation [1], we can eliminate the boson operator and obtain the effective interaction between the two electron spins. Former research mainly focused on the case where $f_1(t)$ and $f_2(t)$ are time independent [23]. However, the time-independent approach may not work well in practice. Now, because of the motion of the tip, we take

the time-dependence of interaction into consideration, namely, $f_1(t)$ and $f_2(t)$ depend on time.

Let us first summarize the main idea of the time-dependent Fröhlich transformation [1] so that our paper is self consistent for reading. Generally speaking, Fröhlich transformation [24, 25] is frequently used in condensed matter physics to obtain effective interaction between two electrons by exchanging virtual phonons. For a quantum system described by Hamiltonian $H(t) = H_0 + H_1(t)$, where H_0 is time independent and $|H_0| \gg |H_1(t)|$, we can make a canonical transformation

$$|\psi(t)\rangle \rightarrow e^{-F(t)}|\psi(t)\rangle, H(t) \rightarrow e^{-F(t)}H(t)e^{F(t)}, \quad (9)$$

where $F(t)$ is an anti-Hermitian operator and $\psi(t)$ the state of the system. When $F(t)$ is appropriately chosen to make the first-order term of the effective Hamiltonian vanishing, i.e., $H_1 + [H_0, F] - i\partial_t F = 0$, we obtain an effective Hamiltonian to the second order $H_{eff} = H_0 + [H_1, F]/2$ in principle, and the above equation explicitly determines $F = F(t)$.

In this section, the canonical transformations are made to obtain the effective Hamiltonian. In the interaction picture with respect to

$$H_0^S = \omega_z(S_z^{(1)} + S_z^{(2)}) + \omega_z(B^+B + \sum_k C_k^+ C_k),$$

the Hamiltonian $H^I = H_0^I + H_1^I + H_p^I$ contains three parts

$$H_0^I = \Delta_1 S_z^{(1)} + \Delta_2 S_z^{(2)}, \quad (10)$$

$$H_1^I = \sum_{i=1,2} f_i \Omega (S_+^{(i)} B + S_-^{(i)} B^+), \quad (11)$$

$$H_p^I = e^{itH_0^S} H_p^S e^{-itH_0^S} \equiv H_p^S \quad (12)$$

Here,

$$\Delta_j = \Omega_z - \omega_z - f_j N g_0 I_0 (j = 1, 2)$$

are the detunings of electron spin and nuclear spin and hyperfine interaction.

It can be observed from the Hamiltonian H^I that the time-dependent term H_1^I can be considered as first-order perturbation with respect to the zeroth-order term H_0^I (disregarding H_p^I). Then, we perform a transformation $\exp(F(t))$ to the Hamiltonian H^I to eliminate the time-dependent term H_1^I , that is, the condition

$$H_1^I + [H_0^I, F] - i\partial_t F = 0 \quad (13)$$

should be fulfilled, where TDFT operator is

$$F(t) = (x_1(t)S_+^{(1)} + x_2(t)S_+^{(2)})B - h.c.$$

It follows from Eq.(13) that the corresponding coefficients of $S_+^{(1)}B$, $S_-^{(1)}B^+$, $S_+^{(2)}B$ and $S_-^{(2)}B^+$ at the left hand side of Eq.(13) vanish, i.e.,

$$\Omega f_1 + \Delta_1 x_1 - i\dot{x}_1 = 0, \quad (14)$$

$$\Omega f_2 + \Delta_2 x_2 - i\dot{x}_2 = 0. \quad (15)$$

In case that the tip is moving from electron 1 towards electron 2 with a uniform speed v , the horizontal position of the tip $R(t) = vt$. Thus, the solutions to the above equations are $x_i \simeq \Omega f_i / \Delta$ ($i = 1, 2$), where $\Delta = \Omega_z - \omega_z$ is used to replace Δ_1 and Δ_2 since $\Delta \simeq \Delta_1 \simeq \Delta_2$ in the realistic parameters (for the necessary details please refer to the Appendix B). Then, the effective Hamiltonian is obtained approximately as follows

$$\begin{aligned} H^F \simeq & H_0^I + \frac{1}{2}[H_1^I, F] + H_p^I + [H_p^I, F] \\ \simeq & [\Delta_1 + \frac{f_1^2}{\Delta} \Omega^2 (2 \langle B^+B \rangle + 1)] S_z^{(1)} \\ & + [\Delta_2 + \frac{f_2^2}{\Delta} \Omega^2 (2 \langle B^+B \rangle + 1)] S_z^{(2)} \\ & + \frac{f_1 f_2}{\Delta} \Omega^2 (S_+^{(1)} S_-^{(2)} + h.c.) + H_p^I + [H_p^I, F], \end{aligned} \quad (16)$$

where $\langle B^+B \rangle$ denotes the average number of nuclear excitation.

When almost all nuclear spins are in their ground state, the system is in the low collective excitation limit, i.e., $\langle B^+B \rangle \rightarrow 0$. By using

$$|\Delta_{1,2}| \simeq |\Delta| \gg \Omega,$$

we have

$$\Delta_j + \frac{\Omega^2}{\Delta_j} f_j^2 (2 \langle B^+B \rangle + 1) \simeq \Delta_j \simeq \Delta.$$

Thus,

$$\begin{aligned} H^F \simeq & \Delta (S_z^{(1)} + S_z^{(2)}) + \frac{\Omega^2}{\Delta} f_1 f_2 (S_+^{(1)} S_-^{(2)} + h.c.) \\ & + H_p^I + [H_p^I, F]. \end{aligned} \quad (17)$$

In the following calculation, it will be shown that the complex term $[H_p^I, F]$ will be dropped in the interaction picture. With respect to $H_0 = \Delta (S_z^{(1)} + S_z^{(2)})$, the effective interaction Hamiltonian is

$$H_{eff} = V_1 + V_2, \quad (18)$$

where

$$\begin{aligned} V_1 = & e^{iH_0 t} [\frac{\Omega^2}{\Delta} f_1 f_2 (S_+^{(1)} S_-^{(2)} + S_+^{(2)} S_-^{(1)})] e^{-iH_0 t} \\ = & \frac{\Omega^2}{\Delta} f_1 f_2 (S_+^{(1)} S_-^{(2)} + S_+^{(2)} S_-^{(1)}), \end{aligned} \quad (19)$$

$$\begin{aligned} V_2 = & e^{itH_0} H_p^I e^{-itH_0} \\ = & g_0 (f_1 S_z^{(1)} + f_2 S_z^{(2)}) (B^+B + \sum_k C_k^+ C_k). \end{aligned} \quad (20)$$

In the above calculation, we have dropped the high-frequency terms $\exp(iH_0 t)[H_p^I, F]\exp(-iH_0 t)$ including the factors $\exp(-i\Delta t)$ or $\exp(i\Delta t)$. It is a reasonable

approximation which is frequently used in the Jaynes-Cummings model.

Now, we study the time evolution driven by the above the effective Hamiltonian. First of all, we study a special case that the total system is initially prepared without the collective excitations of the bus spins. In this case, the effective interaction V_2 does not play a role. In a Hilbert space spanned by the two electron states $|ee\rangle$, $|eg\rangle$, $|ge\rangle$ and $|gg\rangle$, it is clear that there exists an invariant subspace spanned by $|eg\rangle$ and $|ge\rangle$. If the system starts from $|\Psi(0)\rangle = |eg\rangle$, at time t it would definitely evolve into

$$|\psi(t)\rangle = \cos \theta(t) |eg\rangle - i \sin \theta(t) |ge\rangle,$$

where

$$\theta(t) = \int_0^t \frac{\Omega^2}{\Delta} f_1(t') f_2(t') dt'. \quad (21)$$

In comparison with the result in Ref.[22], where H_p was considered as a perturbation in the low excitation approximation, we examine the system evolving under total Hamiltonian containing V_1 and V_2 . Then we can get the equations for the coefficients as follow

$$i\dot{C}_{ge} = \frac{\Omega^2}{\Delta} f_1 f_2 C_{eg} - (V_2)_{eg} C_{ge}, \quad (22)$$

$$i\dot{C}_{eg} = (V_2)_{eg} C_{eg} + \frac{\Omega^2}{\Delta} f_1 f_2 C_{ge}, \quad (23)$$

where $(V_2)_{jk} = \langle jk|V_2|jk\rangle$ and $j, k = e, g$. Similarly, there's an invariant subspace $\{|eg\rangle, |ge\rangle\}$.

IV. SPIN ENTANGLEMENT

In the above sections, we have obtained a typical spin-spin coupling in the effective Hamiltonian, which is induced by the tip excitations. Driven by this Hamiltonian, two electron spins can be entangled dynamically. To characterize the extent of entanglement, we use concurrence to measure the induced entanglement. Actually, even from the original Hamiltonian (1) we can also prove that the corresponding reduced density matrix for two spin is of the form (see the Appendix C).

$$\rho^{(ij)} = \begin{pmatrix} u^+ & 0 & 0 & 0 \\ 0 & w^1 & z^* & 0 \\ 0 & z & w^2 & 0 \\ 0 & 0 & 0 & u^- \end{pmatrix}. \quad (24)$$

This general form is consistent with that obtained straightforwardly from the effective Hamiltonian given in the last section.

For an arbitrary state of two-qubit system described by the density operator ρ , a measure of entanglement can be defined as the concurrence [27, 28],

$$C(\rho) = \max\{0, \lambda_1 - \lambda_2 - \lambda_3 - \lambda_4\}, \quad (25)$$

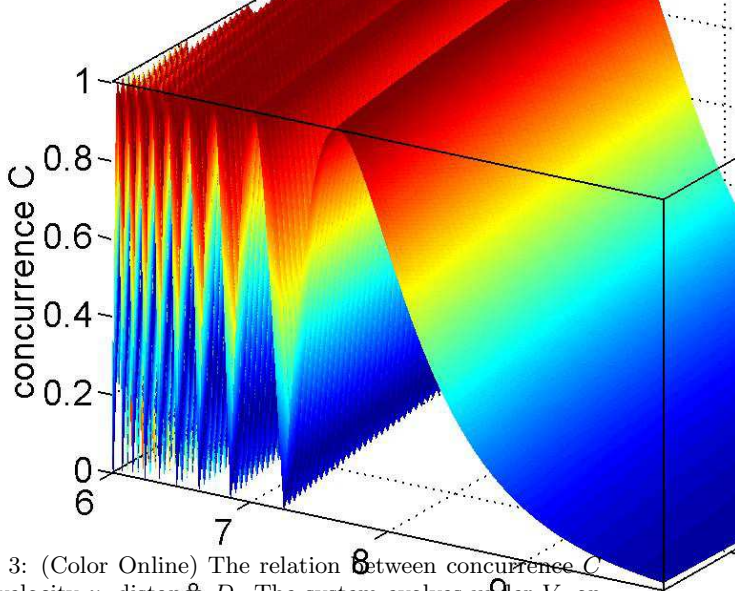


FIG. 3: (Color Online) The relation between concurrence C and velocity v , distance D . The system evolves under V_1 on condition that $x = 10$ nm, $N = 100$, $\alpha = 0.2$ nm $^{-1}$, $\Delta = 1$ MHz, $g_0 \simeq 120$ Hz, $I_y = 10^{12}$ A.
 horizontal distance D (m)

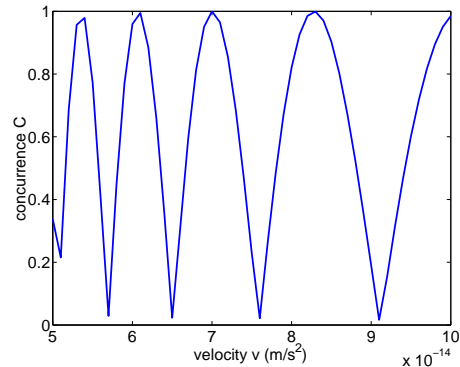


FIG. 4: Sectional view of Fig.3 where the distance $D = 60$ nm.

where the λ_i 's are the square roots of the eigenvalues of the non-Hermitian matrix $\tilde{\rho}$ in decreasing order. And

$$\tilde{\rho} = (\sigma_y \otimes \sigma_y) \rho^* (\sigma_y \otimes \sigma_y),$$

where ρ^* is the complex conjugate of ρ , σ_y the Pauli operator.

A. Time evolution driven by V_1

We investigate the concurrence of the two spins after the tip has arrived above electron 2 at a uniform speed v . In Fig.3, the concurrence is plotted while the speed v and the horizontal distance between the two spins D are varied. It is obvious that the concurrence fluctuates from 0 to 1 in the low speed region. When the tip moves with a relative low speed, the concurrence oscillates rapidly since a lower speed means more time for evolution from a direct product state towards an entangled state. As the speed increases, the concurrence falls monotonously if it is bigger than a certain value. And the maximum

entangled state can be obtained when

$$\theta = (n + 1)\frac{\pi}{4} \quad (26)$$

in Eq.(21). However, the relation between the concurrence and D is a little more complicated. Likewise, a longer distance D gives more time for evolution. On the other hand, the matrix elements of V_1 drop dramatically as D increases.

B. Decoherence and Different Motion Types

In the last section, we have assumed the tip moves with a uniform speed. However, it is very interesting to investigate system evolution for different motions of the tip, e.g., accelerated motion and harmonic oscillation.

In a uniformly accelerated motion, the tip starts above electron 1 with an original speed v_0 and finally stops above electron 2. During the process of moving, its velocity decreases with an acceleration a and hence at time t the horizontal position of the tip is also time dependent, that is,

$$R(t) = v_0 t - \frac{1}{2} a t^2. \quad (27)$$

In a harmonic oscillation, the tip also starts from electron 1 and stops at electron 2, while its position is

$$R(t) = \frac{D}{2}(1 - \cos \omega t). \quad (28)$$

To make a comparison among them, we assume the times for these three motions are equal and thus we have

$$\begin{aligned} v_0 &= 2v, \omega = \frac{\pi v}{D} \\ a &= \frac{v_0}{t} = \frac{2v^2}{D}. \end{aligned}$$

In Fig.5, we plot the concurrence evolution of the three motion types under V_1 . As shown in the figure, there is no great difference among them. The concurrence of different motion types increases linearly since the only effect of V_1 is driving an initial direct product state into an entangled state. However, a different result takes place when we consider a system evolving under $H_{eff} = V_1 + V_2$ as shown in Fig.6. It appears that the concurrence for the uniform motion and accelerated motion increases rapidly in the first half process and arrives at a steady value after several period of oscillation. On the contrary, the concurrence for the harmonic oscillation remains at a relative low level all the time.

To see the essence why different motion types of the tip place different influence on the result, we analyze the spatial dependence of the effective Hamiltonian. As mentioned above, V_1 is off-diagonal and its only influence on the system is entangling the two electron spins. However, V_2 , which is diagonal, can only lead to a phase shift. At

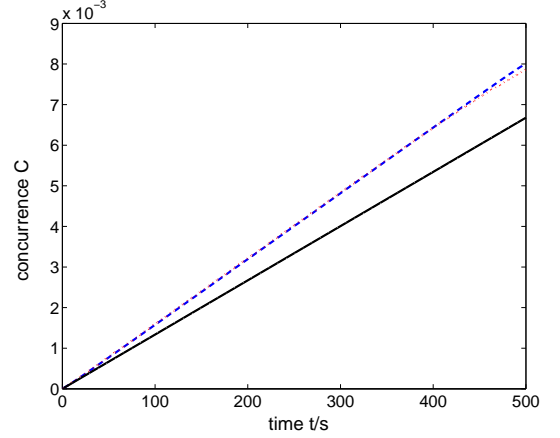


FIG. 5: (Color Online) The relation between concurrence C and motion type under V_1 . The system evolves under $H_{eff} = V_1$ on condition that $d = 1$ nm, $N = 100$, $\alpha = 0.2$ nm $^{-1}$, $\Delta = 1$ MHz, $g_0 \simeq 120$ Hz, $I_0 = 1/2$. Blue dashed line for uniform motion, red dotted line for accelerated motion, and black line for harmonic oscillation.

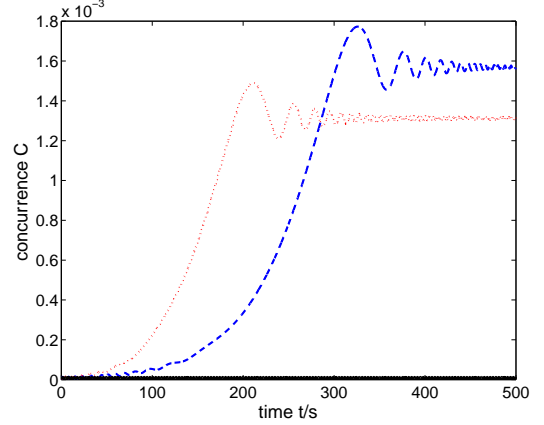


FIG. 6: (Color Online) The relation between concurrence C and motion type under $H_{eff} = V_1 + V_2$. The system evolves under V_1 on condition that $d = 1$ nm, $N = 100$, $\alpha = 0.2$ nm $^{-1}$, $\Delta = 1$ MHz, $g_0 \simeq 120$ Hz, $I_0 = 1/2$, $B^+B + \sum_k C_k^+ C_k = 0.01$. Blue dashed line for uniform motion, red dotted line for accelerated motion, and black line for harmonic oscillation.

the beginning and finishing stages of the motion, the V_2 predominates in the effective Hamiltonian while V_1 replaces V_2 between times. Therefore, the concurrence for the harmonic oscillation stays low since it moves with a low speed at both ends while with a high speed in between. In contrast to this situation, the counterparts for the other two motions can increase to a relative high value as there is no significant variation between the velocity at both ends and in the midway.

V. CONCLUSION

In this paper, we propose a protocol to entangle two electron spins by moving a magnetic tip. We also study the influence of different spatial motion types of the tip on the entanglement of the system. Theoretically, the maximum entangled state can be obtained if the tip moves in a suitable way. However, this protocol may not work well in practice since the relaxation time of electrons in the solid-state systems is much shorter than that is needed in this protocol.

Thus, more progress in experiment improving relaxation time of the confined electron is still needed to put this protocol into practice. Once the effective Bohr radius a of the electrons in semiconductors drops by an order of magnitude, the hyperfine interaction constant g_0 will be increased by three orders of magnitude. Moreover, along with the reduction of a , the distance between two electrons can also be decreased. As a result, the operating time for this protocol will be greatly reduced. Further improvement can also be introduced if all nuclear spins are prepared in their ground state when the tip is cooled to sufficient low temperature.

Actually, there are only the internal collective excitations considered as the quantum data bus to coherent link two spins so that induced the inter-spin entanglement. If there existed the un-expected spatial oscillations of the tip with higher widely-distributed frequencies (, which behave as a white noise) then extra decoherence will be induced to break our protocol presented in this paper. However, if we can cool the tip as a nano-mechanical resonator vis some new mechanism [16], the spatial oscillation of tip well peaked off-resonance will also play the role of the coherent data bus. The most recent experiments about cooling of oscillating mirrors will motivated investigations in forthcoming papers.

Acknowledgement

Thanks very much for helpful discussion with Peng Zhang, Nan Zhao, Zhangqi Yin, Zhensheng Dai, Yansong Li. This work is supported partially by the 973 Program Grant Nos. 2006CB921106, 2006CB921206 and 2005CB724508, National Natural Science Foundation of China, Grant Nos. 10325521, 60433050, 60635040, 10474104, and 90503003.

APPENDIX A: DERIVATION OF $g_1^{(i)}$ AND $g_2^{(i)}$

According to Ref.[26], the hyperfine interaction constant is proportional to the electron spin density located at the nucleus. Thus,

$$g_1^{(i)} = \frac{2\mu_0}{3\hbar} g_e \beta_e g_n \beta_n \left| \psi_1(\vec{R}_{c1} + \vec{r}_i) \right|^2, \quad (A1)$$

where μ_0 is vacuum permeability, g_e and g_n Lande g-factor for the electron and the nucleon respectively, β_e the Bohr magneton, β_n the nuclear magneton, $\psi_1(\vec{r})$ the wavefunction for electron 1. Here, we assume that the wavefunction is s-like since the electron in the quantum dot is at the bottom of the conduction band, that is

$$\left| \psi_1(\vec{R}_{c1} + \vec{r}_i) \right|^2 = \frac{1}{\pi a^3} e^{-\alpha |\vec{R}_{c1}(t) + \vec{r}_i|}, \quad (A2)$$

where $\alpha = 2/a$, a is the Bohr radius for the electron in the quantum dot, $\vec{R}_{c1}(t)$ and $\vec{R}_{c1}(t) + \vec{r}_i$ the positions of the tip center and i 'th nuclear spin with respect to electron 1 respectively.

Using the homogeneous condition that $|\vec{R}_{c1}(t)| \gg |\vec{r}_i|$, one has

$$\begin{aligned} g_1^{(i)} &= g_0 e^{-\alpha |\vec{R}_{c1}(t) + \vec{r}_i|} \\ &\simeq g_0 e^{-\alpha |\vec{R}_{c1}(t)| (1 + \frac{\vec{R}_{c1} \cdot \vec{r}_i}{|\vec{R}_{c1}(t)|^2} + \frac{1}{2} \frac{\vec{r}_i^2}{|\vec{R}_{c1}(t)|^2})} \\ &\simeq g_0 f_1(t), \end{aligned} \quad (A3)$$

where

$$g_0 = 2\mu_0 g_e \beta_e g_n \beta_n / 3\pi\hbar a^3$$

is the hyperfine interaction constant when the nuclear spin is located at the center of the electron's wave function, and

$$f_1(t) = \exp(-\alpha |\vec{R}_{c1}(t)|).$$

According to Ref. [26], in a typical semiconductor, e.g., GaAs, one has

$$a = m\varepsilon a_0 / m^* = 0.052 \times m\varepsilon / m^* \text{nm} \simeq 10 \text{nm}$$

and hence $g_0 \simeq 120$ Hz on condition that

$$g_e \simeq 1, g_n \simeq 1, m^*/m \simeq 0.05, \varepsilon \simeq 10$$

(where a_0 is Bohr radius for hydrogen atom, m_e the mass of free electron, m^* and ε the effective mass and relative dielectric constant for the electron in the quantum dot).

Similarly, we have

$$g_2^{(i)} \simeq g_0 f_2(t), \quad (A4)$$

where

$$f_2(t) = e^{-\alpha |\vec{R}_{c2}(t)|}.$$

APPENDIX B: DERIVATION OF x_i IN UNIFORM MOTION

According to Eq.(14), one has

$$\begin{aligned} x_1 &= -i\Omega e^{-i \int_0^t \Delta_1 dt'} \int_0^t f_1 e^{i \int_0^{t'} \Delta_1 dt''} dt' \\ &\simeq -i\Omega e^{-i\Delta t} \int_0^t f_1 e^{i\Delta t'} dt' \\ &\simeq -i\Omega e^{-i\Delta t} \int_{-\infty}^t f_1 e^{i\Delta t'} dt'. \end{aligned} \quad (B1)$$

Here, we have replaced Δ_1 by $\Delta = \Omega_z - \omega_z$ since

$$f_1 N g_0 I_0 \lesssim 4.8 \text{ kHz} \ll \Delta = 1 \text{ MHz}$$

(since

$$N = 100, I_0 = 1/2, g_0 \simeq 120 \text{ Hz},$$

and

$$f_1 \lesssim \exp(-\alpha d) \simeq 0.8$$

for

$$\alpha = 2/a = 0.2 \text{ nm}^{-1}, d = 1 \text{ nm}$$

). Furthermore, we extend the low limit of the integral range from $t = 0$ to $t = -\infty$ for the reason that the above integral between $t = -\infty$ to $t = 0$ is negligible tiny.

Then one proceeds to have

$$\begin{aligned} x_1 &= \frac{-\Omega}{\Delta} e^{-i\Delta t} (f_1 e^{i\Delta t'}|_{-\infty}^t - \int_{-\infty}^t e^{i\Delta t'} df_1) \\ &= \frac{-\Omega}{\Delta} e^{-i\Delta t} (f_1 e^{i\Delta t} + \int_{-\infty}^t \alpha \frac{v^2 f_1 e^{i\Delta t'} t'}{\sqrt{d^2 + (vt')^2}} dt') \\ &\simeq \frac{-\Omega}{\Delta} e^{-i\Delta t} (f_1 e^{i\Delta t} + \int_{-\infty}^t \alpha \frac{v}{\frac{1}{\alpha}} f_1 e^{i\Delta t'} dt'). \end{aligned} \quad (\text{B2})$$

In the above calculation, we have replaced

$$\int_{-\infty}^t \alpha \frac{v^2 t' f_1(t') e^{i\Delta t'}}{\sqrt{d^2 + (vt')^2}} dt'$$

by

$$\int_{-\infty}^t \alpha \frac{v}{\frac{1}{\alpha}} f_1(t') e^{i\Delta t'} dt',$$

since one notices the fact that $vt' \sim 1/\alpha$ is the effective integration range and the change of $f_1(t')$ (also change of vt') is much slower than that of $e^{i\Delta t'}$.

$$\begin{aligned} x_1 &= \frac{-\Omega}{\Delta} e^{-i\Delta t} (f_1 e^{i\Delta t} + \alpha v \int_{-\infty}^t f_1 e^{i\Delta t'} dt') \\ &\simeq \frac{-\Omega}{\Delta} f_1 - i \frac{\alpha v}{\Delta} x_1, \end{aligned} \quad (\text{B3})$$

Moreover, similar approximation is also applied to the calculation of x_2 .

$$x_2 \simeq \frac{-\Omega}{\Delta} f_2 + i \frac{\alpha v}{\Delta} x_2, \quad (\text{B4})$$

Generally speaking, Δ depends on the applied magnetic field. In case that $\Delta = 1 \text{ MHz}$ and $1/\alpha = 5 \text{ nm}$, we have $\alpha v/\Delta \ll 1$ for all $v \ll 5 \times 10^{-3} \text{ m/s}$. Therefore,

$$x_1 \simeq \frac{-\Omega f_1}{\Delta}, x_2 \simeq \frac{-\Omega f_2}{\Delta}. \quad (\text{B5})$$

APPENDIX C: CONCURRENCE AND REDUCED DENSITY MATRIX

We consider that, in the original Hamiltonian the interaction terms

$$\begin{aligned} H_I &= S_z^{(1)} \sum_{j=1}^N g_1^{(j)} I_z^{(j)} + S_z^{(2)} \sum_{j=1}^N g_2^{(j)} I_z^{(j)} \\ &\quad + S_+^{(1)} \sum_{l=1}^N \frac{g_1^{(j)}}{2} I_-^{(j)} + S_+^{(2)} \sum_{j=1}^N \frac{g_2^{(j)}}{2} I_-^{(j)} + h.c., \end{aligned} \quad (\text{C1})$$

conserves the total spin z-component

$$S_z = \sum_{j=1}^N I_z^{(j)} + S_z^{(1)} + S_z^{(2)}$$

i.e., $[H_I, S_z] = 0$. For such conserved system we express the concurrence characterizing quantum entanglement in terms of observables, such as correlation functions.

The complete basis vectors of the total system are denoted by

$$\begin{aligned} |S_1, S_2, \{I_j\}\rangle &= |S_1, S_2; I_1, \dots, I_N\rangle \\ &= \prod_{j=1}^N |I_j\rangle \otimes |S_1\rangle \otimes |S_2\rangle \end{aligned} \quad (\text{C2})$$

where $|I_j\rangle$ is nuclear spin state and $|S_{1,2}\rangle$ denote the electronic spins ($I_j, S_{1,2} = 0, 1$) respectively. The fact that S_z is conserved can be reflected by the vanishing of some matrix elements of the density operator $\rho = \rho(H)$ on the above basis for any state of the total system, that is,

$$\rho_{S_1, S_2; I_1, \dots, I_N}^{S'_1, S'_2; I'_1, \dots, I'_N} = \rho_{\{n_j, s_j\}}^{\{n_j, s_j\}} \delta(s, s', I, I'), \quad (\text{C3})$$

where

$$\delta(s, s', I, I') = \delta(S_1 + S_2 - S'_1 - S'_2 + \sum_{j=1}^N (I_j - I'_j))$$

The functional $\rho(H)$ of the Hamiltonian may be a ground state or thermal equilibrium states. The reduced density matrix $\rho^{(12)} = \text{Tr}_I[\rho(H)]$ for two atomic quasi-spins, e.g., s_1 and s_2 are obtained as

$$[\rho^{(12)}]_{S_1, S_2}^{S'_1, S'_2} = \delta(s, s', 0, 0) \sum_{\{I_j\}} \rho_{S_1, S_2; I_1, \dots, I_N}^{S'_1, S'_2; I_1, \dots, I_N} \quad (\text{C4})$$

by tracing over all nuclear variables. The corresponding reduced density matrix for two atoms i and j is of the form

$$\rho^{(ij)} = \begin{pmatrix} u^+ & 0 & 0 & 0 \\ 0 & w^1 & z^* & 0 \\ 0 & z & w^2 & 0 \\ 0 & 0 & 0 & u^- \end{pmatrix}.$$

According to Refs. [27, 28], the concurrence $C_{ij} = \max\{0, \lambda_1 - \lambda_2 - \lambda_3 - \lambda_4\}$ for two spin subsystem is obtained in terms of the square roots $\{\lambda_i\}$ ($\lambda_1 = \max\{\lambda_i\}$) of eigenvalues of the non-Hermitian matrix $\rho\tilde{\rho}$. Here

$$\tilde{\rho} = (\sigma_y \otimes \sigma_y) \rho^* (\sigma_y \otimes \sigma_y). \quad (\text{C5})$$

Using the observable quantities, the quantum correlation

$$\begin{aligned} z &= \langle \psi | S_1^+ S_2^- | \psi \rangle, \\ u^\pm &= \langle \psi | (1/2 \pm S_1^z) (1/2 \pm S_2^z) | \psi \rangle, \end{aligned} \quad (\text{C6})$$

the concurrence is rewritten as a computable form

$$C_{ij} = 2 \max(0, |z| - \sqrt{u^+ u^-}). \quad (\text{C7})$$

We note that this formula for the concurrence of two electron spins in the coupled system is the same as that for a spin-1/2 coupling system modeled by the effective Hamiltonian [27, 28].

[1] Yong Li, C. Bruder, and C. P. Sun, Phys. Rev. A, in press (2007).
[2] P. W. Shor, in *Proceedings of the Symposium on the Foundations of Computer Science, 1994, Los Alamitos, California* (IEEE Computer Society Press, New York, 1994), pp. 124-134.
[3] L. K. Grover, Phys. Rev. Lett. **78**, 325-328 (1997).
[4] L. Long, Phys. Rev. A **64**, 022307 (2001).
[5] D. Loss, and D. P. DiVincenzo, Phys. Rev. A **57**, 120 (1998).
[6] B. E. Kane, Nature **393**, 133 (1998).
[7] Y. Manassen, I. Mukhopadhyay, and N. R. Rao, Phys. Rev. B **61**, 16223 (2000).
[8] G. P. Berman, G. W. Brown, M. E. Hawley, and V. I. Tsifrinovich, Phys. Rev. Lett. **87**, 097902 (2001).
[9] G. P. Berman, G. D. Doolen, P. C. Hammel, and V. I. Tsifrinovich, Phys. Rev. Lett. **86**, 2894 (2001).
[10] G. L. Long, Y. J. Ma, and H. M. Chen, Chin. J. Semiconductor, **24**, Suppl. May, 43 (2003).
[11] X. M. H. Huang, C. A. Zorman, M. Mehregany and M. L. Roukes, Nature **421**, 496 (2003).
[12] A. N. Cleland and M. R. Geller, Phys. Rev. Lett. **93**, 070501, (2004).
[13] A. Gaidarzhy, G. Zolfagharkhani, R. L. Badzey and P. Mohanty, Phys. Rev. Lett. **94**, 030402 (2005).
[14] A. Gaidarzhy, G. Zolfagharkhani, R. L. Badzey and P. Mohanty, Appl. Phys. Lett. **86**, 254103 (2005).
[15] F. Xue, L. Zhong, Y. Li, and C. P. Sun, Phys. Rev. B **75**, 033407 (2007).
[16] P. Zhang, Y. D. Wang and C. P. Sun, Phys. Rev. Lett. **95**, 097204 (2005).
[17] D. Gammon, Al. L. Efros, T. A. Kennedy, M. Rosen, D. S. Katzer, and D. Park, Phys. Rev. Lett. **86**, 5176 (2001).
[18] K. Ramaswamy, S. Mui, and S. E. Hayes, Phys. Rev. B **74**, 153201 (2006).
[19] A. V. Balatsky, J. Fransson, D. Mozyrsky, and Yishay Manassen, Phys. Rev. B **73**, 184429 (2006).
[20] Andre R. Stegner, Christoph Boehme, Hans Huebl, Martin Stutzmann, Klaus Lips and Martin S. Brandt, Nature Physics. **2**, 835 (2006).
[21] J. M. Taylor, C. M. Marcus, and M. D. Lukin, Phys. Rev. Lett. **90**, 206803 (2003).
[22] Z. Song, P. Zhang, T. Shi, and C. P. Sun, Phys. Rev. B **71**, 205314 (2005).
[23] S-B Zheng, and G-C Guo, Phys. Rev. Lett. **85**, 2392 (2000).
[24] H. Fröhlich, Phys. Rev. **79**, 845 (1950); Proc. Roy. Soc. A **215**, 291 (1952); Adv. Phys. **3**, 325 (1954).
[25] S. Nakajima, Adv. Phys. **4**, 463 (1953).
[26] A. Schweiger, and G. Jeschke, *Principles of Pulse Electron Paramagnetic Resonance*, (Oxford University Press, Oxford, 2001).
[27] W. K. Wootters, Phys. Rev. Lett. **80**, 2245 (1998).
[28] X. Wang and P. Zanardi, Phys. Lett. A **301**, 1 (2002); X. Wang, Phys. Rev. A **66**, 034302 (2002).
[29] D. Kleckner and D. Bouwmeester, Nature **444**, 75 (2006); A. Naik et al., Nature **443**, 193 (2006); S. Gigan et al., Nature **444**, 67 (2006); O. Arcizet et al., Nature **444**, 71 (2006); M. Poggio, cond-mat/0702446